A temporal map of division, chromatin modification, and identity specification in the regenerating root.

Abstract

Plants have a remarkable capacity for regeneration. In *Arabidopsis thaliana* (Arabidopsis), the entire root tip—housing stem cells and specialized cells like the gravity-sensing columella—can be cut off and the remnant tissue will rapidly divide and differentiate to replace these missing identities. Despite some knowledge of the molecular mechanisms driving this process, the necessity of cell division in this context is not fully understood. Here, we define a timeline of the major steps in regeneration and investigate the role of division and chromatin remodeling in that time. We show that while cell cycle inhibition blocks regeneration, some partial reprogramming can still occur. We outline three broad processes during regeneration—ectopic stem cell niche gene expression, loss of remnant identities, and gain of new identities—and show that some reprogramming events like ectopic stem cell niche gene expression are division-independent. We find that the cell cycle is also accelerated during root regeneration, speeding up to nearly three times faster than in uncut roots. Moreover, we show that histone deacetylase (HDAC) activity is critical at the very early stages of regeneration, potentially preceding the role of cell division. Intriguingly, a one-hour treatment with the HDAC inhibitor Trichostatin A (TSA) immediately upon root tip removal is sufficient to significantly perturb regeneration, whereas a one-hour cell cycle inhibition is not. We propose that Class I HDACs are the prime mediators of this HDAC inhibition and implicate *HDA19* as a potential regulator of early reprogramming in root tip regeneration.

Introduction

Absent motility, plants have evolved a high degree of plasticity in reacting to their environment. From optimized lateral root and root hair growth to capitalize on nutrient-rich patches of earth (Ruffel et al., 2011) to non committal cell fate decisions that allow rapid replacement of damaged neighboring tissues (Kidner et al., 2000), plant cells are remarkably flexible. This flexibility is also apparent at the organismal level in the form of meristems—regions of active cell division and differentiation that constantly give rise to new organs and harbor stem cells (Kidner et al., 2000; Weigel and Jürgens, 2002).

A defining property of stem cells is their division pattern: one daughter stays undifferentiated while the other goes on to differentiate. We previously showed that, in *Arabidopsis thaliana* (Arabidopsis), normal stem cell activity may not be needed for regeneration (Sena et al., 2009). In fact, many cells could function as temporary stem cells to propagate tissues (Efroni et al., 2016), with cell division a potentially necessary step in reprogramming.

But what is it about cell division that allows reprogramming to occur? Passage through the cell cycle seems to be a crucial step for at least some developmental processes. For one, division is an opportunity for cells to reset their chromatin state, allowing them to change fates. In the root epidermis, where hair and non hair cells form an alternating pattern (Costa and Shaw, 2006), the transcription factor GLABRA2 (GL2) is expressed in differentiating non hair cells (Costa and Shaw, 2006). Interestingly, if hair cells are displaced from a hair file into a non hair file, they change identity, in part by actively reorganizing chromatin around the *GL2* locus during G_1 (Costa and Shaw, 2006). A similar dependence of cell fate on division is seen in the floral meristem, where terminal differentiation of floral stem cells relies on eviction of Polycomb group proteins through dilution by division (Sun et al., 2014).

Different phases of the cell cycle come with varying levels of competence to receive and/or respond to developmental cues. For instance, in the embryonic hypophysis (the precursor cell to the quiescent center, or QC), progression rate through the cell cycle is tightly regulated, and deviations from the normal cell cycle length result in patterning defects (Jenik et al., 2005). Similarly, in the sepal, concentration of the transcription factor ATML1 fluctuates randomly over a field of identical epidermal cells; cells in which its levels surpass a certain level during G_2 phase of their cell cycle are committed to giant cell fate and begin endoreplicating, whereas the rest divide (Meyer et al., 2017).

Cell division can also allow cells to differentially partition cell fate determinants, like in the stomatal lineage in leaves (Dong et al., 2009). There, unequal distribution of the protein BASL is associated with early asymmetric divisions. Later, nuclear vs peripheral localization of BASL in the daughters of these divisions correlates with specific cell fates, such as continued asymmetric cell division or terminal differentiation (Dong et al., 2009).

There are also cases where division is not needed for cell fate specification, such as in male gametophyte development, where one generative cell divides to generate two sperm cells (Iwakawa et al., 2006). In mutants where this division does not occur, the single undivided generative like cell is still capable of fertilization (Iwakawa et al., 2006), showing that a functional cell fate can nonetheless be established without division.

Division and differentiation are tightly coupled, making it difficult to study the dependence of one on the other. Regeneration as an experimental system gets around this limitation by dramatically resetting organ development in an adult context. So while in the root apical meristem homeostatic growth necessarily couples division and identity specification, regeneration can uncouple these two processes, allowing closer study.

Animal regeneration models provide some insights into the role of cell division in regeneration specifically, with non lineage restricted identity transitions, accelerated cell cycles, and histone modifications all being features (Sánchez Alvarado, 2009). For instance, fin regeneration in zebrafish proceeds via rapid proliferation of mesenchymal cells once the wound epithelium and blastema are established (Pfefferli and Jaźwińska, 2015).

Chromatin regulation at the histone level has also been implicated in fin regeneration, with demethylation of a repressive H3K27me3 mark (Pfefferli and Jaźwińska, 2015), as well as deacetylation of histone tails via the activity of histone deacetylase 1 (Pfefferli et al., 2014) both being required. Repressive H3K27me3 marks are catalyzed by Polycomb Repressive Complex 2 (PRC2), which has been implicated in inhibiting dedifferentiation in mature cells in both the Arabidopsis root (Ikeuchi et al., 2015) and shoot (Ohashi-Ito and Bergmann, 2006).

The interplay between differentiation state, chromatin modification, and mitotic activity is complex, and all three likely influence one another. Indeed, the concept of dedifferentiation as it was initially conceived necessarily implied active cell division (emphasis ours): “the release of living cells from the confines of their previous organization with *accompanying active mitosis* of these cells” (Hay and Fischman, 1961).

Here we show that in Arabidopsis root tip regeneration, cell division is important for loss of remnant identities as well as for gain of new cap identities during reprogramming. Intriguingly, we find that quiescent center early stem cell markers are rapidly restored in a division independent manner. In one of the earliest requirements in regeneration, a one-hour inhibition was enough to severely inhibit regeneration. We propose a model in which early in regeneration—within a few hours—early regulators / stem cell markers are broadly expressed. Through recruitment of histone deacetylases (HDACs), remnant identities near the cut site are suppressed to allow for further reprogramming into new cell types. We implicate *HDA19* as a potential early positive regulator of this process.

Results

Identification of a regeneration specific transcriptional program

Arabidopsis roots are able to rapidly replace lost or damaged tissues, even when the entire tip of the root—containing QC, columella, lateral root cap (LRC), and all initials—is surgically removed (**Figure 1a**). We previously showed that cells early in this process take on mixed or chimeric transcriptional identities before eventually differentiating (Efroni et al., 2016). To study these identity transitions more closely, we performed single cell RNA sequencing (scRNA-seq) at 4, 9, 14, 24, and 36 hours post cut. Cells from uncut roots of the same age were used as a reference dataset against which to align cells from cut roots. Gene expression was normalized using the SCTranform approach instead of the default log

normalization (Hafemeister 2019) as this approach forces each cell from the cut condition to align onto the reference according to their transcriptome in an unsupervised way. In total, 30,657 cells were sequenced and combined using the R package Seurat (Satija et al., 2015). The resulting clusters were annotated based on published datasets from our lab as well as more recently published scRNA-seq data (**Figure 1b**).

To identify cells that have a transcriptomic signature unique to regeneration, we used a topic modeling approach. In this approach, each cell's transcriptome can be summarized as a combination of K number of topics in varying proportions, where each topic is composed of hundreds of genes that are coexpressed. We performed topic modeling analysis on cells in both cut and uncut conditions using the R package CountClust (Dey et al., 2017) and a total of K=11 topics. Of these 11 topics, one—topic No. 4—was enriched in cut cells and almost totally absent from uncut cells (**Figure 1c, Supplemental Figure 1a**). A closer look at the genes making up this topic revealed many known transcriptional regulators of root development such as *PLETHORA1* (*PLT1*), *PLETHORA2* (*PLT2*), *WOODENLEG* (*WOL*), *SCARECROW* (*SCR*), *BABYBOOM* (*BBM*), *ROOT GROWTH FACTOR 2* (*RGF2*), and *ROOT GROWTH FACTOR 3* (*RGF3*) (Motte et al., 2019). In total, we found 3,677 cells with a high proportion of topic No. 4, compared to only 130 cells in the uncut.

To identify the tissues from which topic No. 4-enriched cells originated, we looked at their distribution within our newly generated time series clusters (**Figure 1d**). Interestingly, at 4 hours, topic No. 4 is enriched in clusters annotated as a mix of closely related *QC*, *initials*, or *endo-cortex* cells. By 9 and 14 hours, this topic is enriched in the *cortex* and *young columella* clusters. And by 24 and 36 hours, it is more or less restricted to cells annotated as *columella* and *LRC*. This suggested that the earliest cells to undergo reprogramming are ground tissue cells left over after injury, which are known to ectopically activate QC specific gene expression. As the root regenerates, these cells mature, taking on transcriptional identities of progressively more mature tissues, before the missing columella and lateral root cap are finally replaced by 36 hours.

Topic modeling also revealed several regeneration-specific marker genes like *WRKY23*, *DOF3.4 (OBP1)* and, *CLE11/12/13* reporter lines, which we subsequently validated by microscopy (**Supplemental Figures 1b-d**).

Single-cell RNA-seq maps the loss and gain of identities during regeneration.

To examine loss of remnant identities, we analyzed how many marker genes were downregulated in each cell type. We found that many cell types, with the exception of epidermis, seem to lose part of their remnant identity, especially at 9, 14, and 24 hours.

Similarly, to test if loss of remnant identities is coupled with a gain of new ones, we examined all differentially upregulated genes in each cell type. We found that many marker genes typically unique to certain tissues were ectopically upregulated in completely different cell types.

Next we wanted to map out the developmental trajectory of cells as they transition through each of our time points in regeneration. Enrichment tests of cell type-specific marker genes induced during the different timepoints revealed that remnant tissues generally contribute to the formation of their outer neighbor in the regenerated root tip, consistent with our previous clonal analysis (Efroni et al., 2016). For example, remnant stele cells give rise to adjacent pericycle and endo-cortex, pericycle gives rise to neighboring endodermis, endodermis gives rise to cortex, and the newly formed columella is derived primarily from remnant stele and ground tissue cells (**Figure 1e**). Interestingly, whereas we did not previously find a significant contribution of remnant epidermis to the regenerating root tip, transcriptional data showed that remnant epidermis does in fact contribute to the formation of newly formed columella and LRC at the late 36 hour time point.

Regeneration after root tip removal comprises three processes: ectopic activation of QC and initial specific gene expression, loss of remnant identities, and gain of new identities (**Figure 2a**). In order to better understand these processes at the transcriptional level, we built a detailed list of unique and shared marker genes across every cell type.

Early stem cell niche related gene expression is division independent.

Upon excising the root tip, the QC and surrounding initials are completely removed. Within a few hours, QC markers return ectopically in a broad domain before gradually focusing to its stable state of a cluster of cells after a few days (Sena et al., 2009). We previously showed that expression of the QC marker *WOX5* returns by 6 hours (Sena et al., 2009). Upon closer examination, *WOX5* expression can be detected as early as 4 hours, primarily in the ground tissue, as seen both by microscopy and scRNA-seq (**Figure 2b**). Given that this timing is shorter than the possible duration of the cell cycle in plants (Zhukovskaya et al., 2018), we examined *WOX5* expression dynamics during regeneration using live imaging to see if ectopic *WOX5* expression occurs before or after mitosis. Time lapse imaging showed that *WOX5* expression appears in cells consistently prior to mitosis (n=7 cells) (**Supplemental Figure 2a, Supplemental Movie 1**).

To validate this live imaging result, we used the thymidine analog 5-ethynyl-2-deoxyuridine (EdU) to label cells that have entered S phase. EdU labeling confirmed the presence of *WOX5* expression in non-divided cells at 4 hours (**Supplemental Figure 2b**). Indeed, even when cutting much higher into the meristem (~200-300 μm from root tip) where roots consistently do not regenerate (Sena et al., 2009), *WOX5* expression is still able to return (**Supplemental Movie 2**). The remnant cells in these higher cuts are in the elongation or differentiation zone, and either postmitotic or terminally differentiated, further suggesting that expression of *WOX5* is division independent.

To more directly test if cell division is necessary for activation of QC specific markers, we treated roots with the Cyclin-Dependent Kinase inhibitor Roscovitine (Planchais et al., 2000). While cell cycle inhibition completely blocks regeneration (**Supplemental Figure 2c**), *WOX5* expression is still able to return even with Roscovitine treatment at both 4 and 24 hours (**Figure 2b**). Another marker of the QC (which additionally marks columella and columella stem cells)—*WIP4*—is also expressed ectopically within a few hours of root tip removal (Efroni et al., 2016). Similar to *WOX5*, *WIP4* expression is unperturbed by cell cycle inhibition (**Figure 2b**). Consistent with this, scRNA-seq analysis of Roscovitine-treated regenerating roots showed both *WOX5* and *WIP4* activation in the presence of Roscovitine. Indeed, more than half of regeneration specific transcription factors are still activated in the presence of Roscovitine.

Taken together, these results suggest that some early events in reprogramming are independent of cell division. Importantly, cell cycle inhibition—while blocking regeneration overall—does not simply freeze general transcription or translation machinery, but rather inhibits specific processes while leaving others intact, as evidenced by the return of *WOX5* and *WIP4*.

Cell cycle inhibition significantly inhibits remnant identity loss.

Immediately after root tip removal, markers of remnant tissues (i.e. stele, ground tissue, epidermis) extend to and are flush with the cut site. But by 18 hours expression is diminished at the distal-most tip of the root, suggesting cells in this region have lost their original identity (**Figure 2c**). To directly test if loss of original identities requires cell division, we examined several transcriptional reporters of remnant identity in regenerating roots after cell cycle inhibition with Roscovitine. At 18 hours, the domains of the endodermal marker *SCARECROW (SCR)*, the cortex marker *CO2*, and the ground tissue marker *J0571* all typically disappear from near the cut site (**Figure 2c**). By comparison, Roscovitine treated roots at the same time point show significantly less disappearance (**Figure 2c**). These results show that a crucial step in reprogramming—loss of former cell identity among specialized cells—is dependent on cell division.

Cell division is required for identities that undergo differentiation

To test if remnant cells can reprogram without dividing, we used live imaging to observe transcriptional reporters of cap identities during regeneration. The expression domain of the columella specific marker *PET111* is completely removed by root tip excision and returns by 24 hours (Efroni et al., 2016). Live imaging showed that *PET111* expression was consistently preceded by mitosis (n=6 cells across 3 time lapse experiments) (**Supplemental Figure 2d, Supplemental Movie 3**). *PET111* is a marker of mature columella cells, so to test an earlier marker of columella identity, we looked at *IAA10*, which is detected as early as 16 hours (Efroni et al., 2016). Similar to *PET111*, *IAA10* expression was only observed following mitosis (n=3 cells from 1 time lapse experiment) (**Supplemental Figure 2e**, **Supplemental Movie 4**). Similarly, the cap domain of the epidermis/LRC marker *WEREWOLF* only appeared after several rounds of division (n=10 cells across 2 time lapse experiments) (**Supplemental Figure 2f, Supplemental Movie 5**).

To directly test the need for cell division in cap identity return, we examined cap specific markers in roots treated with Roscovitine. Roscovitine treatment completely inhibited return of the cap identity markers *PET111*, *IAA10*, and *SOMBRERO (SMB)* (**Figure 2d**, **Supplemental Figure 3a**). Analysis of scRNA-seq data from Roscovitine treated roots similarly showed that cap specific genes such as *BRAVO*, *PLT1*, *TCP20*, *TMO6*, *WRKY21* and *CDF4* are inhibited in the presence of Roscovitine.

Weaker cell cycle inhibition via treatment with Aphidicolin or Hydroxyurea leads to reduced cell cycle entry and concomitant reduction in the number of cells that take on new cap identities (**Supplemental Figure 3b-c**). Importantly, new GFP expression always colocalized with EdU labeling in instances where identity did manage to return (**Supplemental Figure 3b-c**).

To rule out the possibility of chemical inhibitors blocking critical early processes rather than division *per se*, we cut roots and allowed them to regenerate for 4 hours before transferring to media containing Roscovitine. As before, Roscovitine treated roots failed to regenerate or restore *PET111* expression (**Supplemental Figure 3d**).

We conclude that cell division is required for gain of new columella and LRC identities during reprogramming, showing that cell identities outside the stem cell niche require cell division for specification and differentiation.

Reprogramming is phased with uniquely rapid divisions.

In tracking cell division events during regeneration, one interesting feature we noted was that cells were dividing at a very rapid rate compared to the same region of the root during normal growth: cell cycle durations during regeneration are accelerated nearly 3 fold, from roughly 21 hours (Rahni and Birnbaum, 2019) to roughly 8 hours (**Supplemental Figure 3e**). Intriguingly, an 8 hour cell cycle is also observed in other organogenesis contexts in Arabidopsis, such as during lateral root formation (von Wangenheim et al., 2017). Rapid cell cycles have been noted in animal systems too, namely in rat gastrulation (Mac Auley et al., 1993), and in reprogramming of induced pluripotent cells by Yamanaka factors where “privileged” induced pluripotent cells that have rapid cell cycles also reprogram more easily (Guo et al., 2014). An accelerated cell cycle is attributed to a shortened G_1 or G_2 phase, a property that may be correlated with self renewal capacity (Orford and Scadden, 2008).

Early ectopic stem cell niche gene expression is independent of (de)acetylation.

To understand the need for (rapid) divisions in regeneration, we next investigated mechanisms that enables cell division to reset fates. For instance, it has been shown that in root epidermal cells, chromatin is reset and remodeled during the cell cycle (Costa and Shaw, 2006). This process could allow cells to adapt to new cellular contexts and could explain one mechanism by which cell division facilitates reprogramming. To investigate whether chromatin regulation is operating in our regeneration context we combined ATAC-seq data from a previously published regeneration dataset (Rymen et al., 2019) with our own previously generated dataset (Hernández-Coronado et al., 2022). We found that cells annotated as *QC/initials* in our single cell clusters (Figure 1b) at 9 and 14 hours are enriched for ATAC peaks,

specifically in columella specific genes (**Supplemental Figure 4a**). That is, in cells with a stem cell-like transcriptional signature, chromatin near genes typically only expressed in columella was opening up, suggesting that the QC-like cells were undergoing an identity transition. Cells left over after root tip removal could be gaining new identities via regulation at the chromatin level, such as modification of histone tails. One such modification that is reset during cell division is histone acetylation, which promotes gene expression by loosening histone-DNA interactions (Rosa et al., 2014).

To determine if histone acetylation plays a role in reprogramming, we took a pharmacological approach. Histone deacetylases (HDACs) remove acetyl groups from histone tails, leading to compacted chromatin. While HDAC activity generally correlates with gene repression, it is counteracted by the activating effect of histone acetyltransferases (HATs) (Rosa and Shaw, 2013). To test if HDAC/HAT activity is necessary for reprogramming, we treated regenerating roots with chemical inhibitors of either HDACs or HATs. Trichostatin A (TSA) is a pan-HDAC inhibitor (Ueda et al., 2017), leading to hyperacetylation of histone tails (Rosa et al., 2014), while the HAT inhibitor Curcumin specifically targets the CBP/p300 HAT family (Balasubramanyam et al., 2004). To test if HDAC and/or HAT activity is necessary for reprogramming, we treated cut roots with TSA or Curcumin and examined markers for the three broad steps in regeneration outlined above (ectopic stem cell niche gene expression, loss of remnant identities, gain of new identities) (Figure 2a).

First, looking at markers of the QC, we found that expression of *WOX5* was unperturbed in either TSA or Curcumin treatment, showing strong ectopic activation at both 4 and 24 hours (**Figure 2b**). Strikingly, the *WOX5* domain in the TSA condition at 24 hours resembles the mock at 4, suggesting that HDAC inhibition leads to a “stalling” of the regeneration process. Indeed, TSA treated roots at 24 hours resemble mock roots at 0 hours (**Supplemental Figure 4b**). While the *WOX5* domain after Curcumin treatment does not remain fully stalled, it does morphologically resemble earlier regeneration stages in controls, and regeneration is delayed overall in this treatment (**Figure 2b, Supplemental Figure 4b**). Next we examined *WIP4* expression in response to TSA and Curcumin and found that, while it was largely unaffected in response to Curcumin, its expression was completely blocked by TSA at 24 hours (**Figure 2b**). This is in contrast to Roscovitine treatment, which did not affect *WIP4* expression (**Figure 2b**), suggesting that while its activation is division-independent, it is HDAC-dependent. This also importantly shows that Roscovitine and TSA have effects that can be uncoupled, and are not simply globally blocking cellular activity or eliciting a stress response.

These results show that the relationship between HDAC/HAT activity and early niche marker activation is complex, with some gene expression proceeding independently of this chromatin modification.

HDAC inhibition completely inhibits remnant identity loss whereas HAT inhibition does not.

After the rapid activation of stem cell niche markers at around 4 hours, the next broad steps in regeneration are the loss of remnant identities and gain of new ones. To test if remnant identity loss is dependent on HDAC/HAT activity we looked at regenerating roots expressing transcriptional reporters for various remnant tissues after treatment with either TSA or Curcumin. Consistent with “stalling” and failure to complete the regeneration program described above for TSA treatment, remnant identity markers such as *SCR, CO2,* and *J0571* show virtually no disappearance in TSA-treated roots compared to mock (**Figure 2c**). Curcumin treatment, on the other hand, allows partial disappearance of these markers (**Figure 2c**). This result further implicates the necessity for HDAC activity at the earliest stages of regeneration.

Specification of new identities requires both HAT and HDAC activity.

In TSA-treated roots, regeneration completely fails, whereas Curcumin-treated roots are significantly delayed in regeneration. To test if these outcomes are due to a failure to specify new cap

identities, we examined several cap markers in roots treated with either TSA or Curcumin. *PET111, SMB,* and *IAA10* all fail to return in TSA treated roots compared to mock (**Figure 2d**). Curcumin treated roots similarly have a significant reduction in the number of roots gaining these markers during regeneration (**Figure 2d**).

TSA has the potential for mildly cytotoxic effects when used in planta (Rosa et al., 2014). To rule out that TSA-induced stalling and failure to regenerate are due to cell cycle inhibition, we combined TSA treatment with EdU labeling. TSA and mock treated roots both showed uniform S phase entry after 24 hours as seen by EdU labeling (**Supplemental Figure 4c**). Moreover, cells clearly mid-mitosis were observed in both conditions, suggesting that neither S phase entry nor mitosis are significantly impaired by TSA.

Given that Curcumin's activity is specific to the CBP/p300 family of HATs (Balasubramanyam et al., 2004), it seemed possible that the partial inhibition of regeneration under this treatment was due to compensation by other HATs. To test this, we also treated cut roots with MB-3, an inhibitor of the GCN5/GNAT/MYST family of HATs (Aquea et al., 2017). In contrast to Curcumin, MB-3 treatment did not lead to any inhibition of regeneration whatsoever, even at a ten-fold higher concentration (**Supplemental Figure 4d**). This points to a specific role for the CBP/p300 family of HATs during root regeneration.

In contrast to the specificity of these HAT inhibitors, TSA is a pan-HDAC inhibitor that affects all HDAC families (Ueda et al., 2017). To examine which class of HDACs are critical for regeneration, we tested several other HDAC inhibitors. Sodium butyrate is a broad-spectrum HDAC inhibitor that targets both Class I and II HDACs (Ueda et al., 2017). Treatment with sodium butyrate inhibits regeneration and leads to a stalled morphology similar to TSA-treated roots, albeit with an abundance of ectopic amyloplasts appearing along the entire root (**Supplemental Figure 4e**). The predicted Class II-specific HDAC inhibitor TMP195 had no effect on regeneration, consistent with reports of this inhibitor's lack of effect in plants (Ueda et al., 2017). Turning to Class I HDACs, we tested MC1293, MGCD-0103 (Mocetinostat), and FK228 (Romidepsin). While MC1293 and Mocetinostat had no effect, even at higher concentrations, Romidepsin treatment inhibited regeneration and led to stalled roots morphologically identical to TSA-treated roots (**Supplemental Figure 4f**). These results suggest that Class I HDACs (HDA6, 7, 9, and 19) could be playing a critical role in reprogramming.

HDA19 Mutants Are Defective in Regeneration

To investigate which HDACs are playing a role in reprogramming, we screened mutants for the Class I HDACs *HDA6* and *HDA19* for regeneration defects. By 48 hours, mutants for all four genes fully regenerated at the same 100% rate as wild type. Indeed, almost every mutant we have tested, when cut "low" (i.e. just above the vascular initials or roughly 100 μm from the root tip) is able to fully regenerate by 48 hours. Still, mutants may show delays and defects at earlier time points that would not be legible at 48 hours, and higher order mutants for core cellular machinery like HDACs would have pleiotropic effects that complicate interpretations of any regeneration phenotype. To examine more subtle regeneration defects in single mutants we used mPS-PI staining as a quantitative measure of regeneration.

By 18 hours, wild type roots consistently accumulate amyloplasts near the cut site, indicating that cells in this region have successfully reprogrammed to replace missing gravity-sensing cap cells (Figure 1a). Amyloplasts can be visualized using mPS-PI staining (Truernit et al., 2008) and by using confocal microscopy, median sections can be taken of regenerating roots allowing us to count the number of amyloplast-positive cells that are present at a given time point.

We tested two *hda19* mutant alleles: *SALK_0277241*, which contains an insertion just upstream of the 5' UTR, and *hda19-3*, which contains an insertion in the first exon. *SALK_0277241* mutants had significantly fewer amyloplast-positive cells at 18h compared to Col-0 wild type (**Figure 3a**). *hda19-3* mutants also had fewer amyloplast-positive cells at 18 hours, although this difference was not statistically significant (**Figure 3b**). The results with these mutants are consistent with TSA treatment, suggesting that HDAC activity and early chromatin closing activity is necessary for root regeneration.

An *hda6* T-DNA mutant (SALK_206997) with an insertion just past the 3' UTR showed no difference in the number of amyloplast-positive cells at 18h compared to wild type (**Figure 3c**). Two other

hda6 mutant alleles, *rts1-1* and *axe1-5* with a 37 bp deletion in Exon 1, and a premature stop codon point mutation after Exon 3, respectively, both strangely had *more* amyloplasts at 18 hours (**Figure 3d**), suggesting faster regeneration compared to wild type. We crossed both these mutant lines into a transcriptional reporter for *SCR*, and measured the amount of remnant identity loss in mutants vs wild type. Consistent with the mPS-PI results, both *rts1-1* and *axe1-5* mutants had a larger disappearance of *SCR* (**Figure 3f-g**). Taken together, these results suggest that *HDA6* may actually be a negative regulator of regeneration.

While *HDA19* and *HDA6* function redundantly in several contexts (Chen and Wu, 2010; Tanaka et al., 2008; Tian et al., 2005; Zhou et al., 2005), they also are known to have opposing roles, for example, in salt stress response (Ueda et al 2017), which may explain the opposite regeneration phenotypes we found here.

Histone deacetylation is critical at the earliest stages of reprogramming.

Interestingly, the total inhibition of remnant identity loss seen after TSA treatment is somewhat in contrast to Roscovitine treatment where only a small amount of remnant identity loss still occurs (Figure 2c). Taken with the observation that *WOX5* expression seems halted at an early point in TSA treatment (Figure 2b), we speculated that HDAC inhibition may be blocking a critical early process in regeneration such that reprogramming is initiated but not completed. To test this, we treated cut roots with TSA, Roscovitine, or Curcumin for only 1 hour before transferring them to standard media to recover and scoring regeneration two days later. Surprisingly, a 1 hour pulse of TSA, but not Roscovitine or Curcumin, is sufficient to perturb regeneration, leading to a mix of failed, stalled, partially, and fully regenerated roots (**Figure 4a, Supplemental Figure 5a-e**). Increased pulse lengths led to eventual total inhibition by TSA and Roscovitine whereas Curcumin treated roots still regenerated (**Supplemental Figure 5a-e**).

TSA is a reversible inhibitor ("Trichostatin A," n.d.), but to confirm that its action is indeed most critical during the first hour of regeneration we delayed the treatment by first cutting roots then waiting 4 hours before treating for 1 hour on TSA followed by recovery. Consistent with an early window of TSA action, this delayed treatment did not affect regeneration (**Figure 4b**). This 1 hour pulse effect was also observable in a failure to lose old identity in the TSA condition, as seen by perdurance of a *SCR* transcriptional reporter after cutting (**Figure 4c**).

We also tested whether a short pulse of Romidepsin would phenocopy treatment with a short pulse of TSA. A 2 hour pulse of TSA resulted in a significant reduction in fully regenerated roots—37% compared to 96% in mock. A 2 hour Romidepsin pulse saw a moderate but not statistically significant reduction in regeneration at 77%, pointing to a potential compensatory mechanism—whereas Class II and other HDACs could still be functioning in Romidepsin treatment, TSA treatment fully abolishes all HDAC activity across Classes (**Figure 4d**). Still, these results implicate Class I HDACs as potential candidates for early regulators of reprogramming during regeneration.

Discussion

During normal growth, cell division and differentiation are coupled, along with growth itself (Harashima and Schnittger, 2010). This makes experimental approaches to understanding any one of these processes particularly challenging, as perturbations of one will necessarily influence the rest. Regeneration, as an experimental system, circumvents this issue by resetting development in an adult context. By forcing cells to reprogram after having already been specified, the timings of division and identity establishment can be unlinked. Still, given the high background mitotic activity in the root meristem, and the ongoing specification of cells prior to the differentiation zone, pharmacological and single cell approaches were needed to further tease apart division and differentiation processes.

Here we showed that, during regeneration, cell division is a necessary feature of both remnant identity loss and *de novo* specification of tissue-specific identities that were removed by cutting. Interestingly, genes implicated in early root specification, such as *WOX5* and *WIP4,* show a rapid return

that is division-independent.

Following root tip excision, the remnant tissue must not only reconstitute lost stem cell activity but replace missing specialized cells such as the columella as well. The root exhibits a great deal of plasticity, with what were previously differentiating cells in the remnant zone able to completely switch identities in order to reassemble neighboring stem cell lineages and in turn the whole root (Efroni et al., 2016). Single cell profiling has shown that many of these reprogramming cells possess a chimeric or mixed identity between 3 to 16 hours (Efroni et al., 2016).

Our working model is that WOX5 (and/or other early factors) are active very early to help “reset” cell fates, by recruiting HDACs and shutting down existing cell fate programs. Later in regeneration, new cell identities are activated, perhaps relying on HAT activity. Thus, whereas HDAC inhibition (with TSA) blocks early stages of regeneration, blocking HAT activity inhibits later phases of regeneration, when new identities are activated.

During regeneration, in addition to establishing division as a precursor to cap identity acquisition, we showed that the cell cycle is accelerated nearly 3 fold compared to cells in the same region in uncut roots. Acceleration of the cell cycle is commonly observed in contexts where new tissues are being differentiated, such as lateral root formation (Hauschild et al 2017) in plants, or gastrulation in rats (Mac Auley et al., 1993). This acceleration is typically achieved by shortening G_1 and/or G_2. Indeed, rapid cell cycles with short G phases are correlated with high programming rates in induced pluripotent stem cells (Guo et al., 2014). Given that a short G_1 phase is correlated with greater self-renewal capacity (Tsubouchi and Fisher, 2013), it is tempting to consider that fast cycling cells in the regenerating root may show a similar propensity for reprogramming. Further work is needed to experimentally test this idea.

Methods

Plant Growth and Maintenance

Seeds of Arabidopsis plants carrying the transgenes *35S::H2B-mRFP1* and *pWOX5::GFP(ER)* (both in Col-0 background) were stratified at 4˚C for 2 days, sterilized, placed on agar plates containing ½ Murashige and Skoog salts (Sigma M5524), 0.5% sucrose, and grown vertically in chambers set to 23˚C and a 16h light / 8h dark cycle (80-90 µmol m^{-2} s^{-1}).

Microsurgery

Removal of root tips was done by our previously published microsurgery protocol (Sena et al., 2009). Briefly, excisions were done roughly 130 µm from the tip of the root, by hand, with a 30G sterile dental needle (ExcelInt) or just above the vascular initials by using a microscalpel (Feather 72045-15) under a dissecting microscope with faux DIC settings to visualize the upper limit of amyloplasts within the root tip.

Live Imaging

Live imaging of regenerating roots was done using a modified version of our previously published protocol for tracking long-term growth in roots (Rahni and Birnbaum, 2019). As the QC and therefore endogenous *WOX5* domain is removed for regeneration studies, the fluorescent region marked by pWOX5:GFP used for tracking is lost. As a workaround, I tested several live dyes with emission profiles outside that of our cell and tissue reporters.

A variety of dyes, including DAPI and the SYTO family of nucleotide labels, were tested. Ultimately the best solution was found to be DiD’ (Life Technologies), a lipophilic, non-toxic live dye designed to adhere to plasma membranes, have slow diffusivity, and persist for several days while retaining bright fluorescence. DiD’ brightly labeled the cut root tip in several clusters, which gradually shrink to discrete, cell-sized punctae that are amenable to tracking. As these punctae can appear at various positions along the root’s radial axis, minor drift can occur during extended periods of acquisition as the drift correction

module selects different reference planes. As such, while the uncut root can effectively be imaged in a fully automated manner, tracking regenerating roots requires frequent manual adjustment to settings or to the microscope stage itself (see detailed Materials/Methods). The first few hours, in particular, are critical and require active on-the-fly adjustment of the microscope controls to ensure successful imaging.

In lieu of the usual QC-localized fluorescent reporter, a fluorescent DiD' cluster can be presented as a single, discrete object for MatrixScreener to track. Once a suitable cluster is found. To localize dyes to the regenerating root tip, we used a modified version of our microsurgery protocol (Sena et al 2009). By dipping the needle in a solution of DiD' before using it to cut away the root tip, the dye can be primarily localized to the cut site.

Pharmacological Treatment

For experiments with cell cycle inhibitors (Roscovitine, Aphidicolin, Hydroxyurea, Oryzalin), and chromatin modifier inhibitors (Trichostatin A, Circumin, and MB-3), and EdU, the chemical in question was added to autoclaved liquid MS media that had been cooled to 50˚C.

EdU Labeling

A modified version of Kazda et al's protocol (Kazda et al., 2016) was used for EdU labeling. Rather than keeping seedlings in the same dish and replacing the solution at each step, a small dedicated petri dish was used for each solution. That is, seedlings were transferred from a petri containing fixative, to one containing wash buffer, and so on. Rather than use a commercial click cocktail solution, I made one from scratch based on a protocol described on ResearchGate. The labeling solution contained the following reagents at the stated final concentrations in PBS: 2 mM Copper(II) Sulfate Pentahydrate (Sigma 12849), 8 μM Sulfo-Cyanine5 Azide (Lumiprobe B1330), and 20 mg/mL L-Ascorbic Acid (Sigma A4544), added to PBS in that order. DAPI counterstaining was done as described by Kazda.

mPS-PI staining

mPS-PI staining was done following (Truernit et al., 2008). Briefly, seedlings are fixed in 10% acetic acid, 50% methanol for at least one hour, or up to several days. Fixed seedlings are rinsed with water, incubated in periodic acid for 1 hour, rinsed again, incubated in Schiff reagent with propidium iodide for 2-3 hours, then incubated overnight in Visikol for Plant Biology as a clearing agent. Cleared seedlings are mounted in Visikol and imaged using a confocal microscope with 561 nm excitation wavelength.

Protoplast Generation

Protoplast isolation was done as previously described (Bargmann and Birnbaum, 2010), with slight modifications. Protoplast solution is made fresh on day of protoplasting: 400 mM/8% mannitol, 20 mM MES hydrate, 20 mM KCl, 20 mM CaCl2, 1.2% Cellulase R10 (Yakult,ONOZUKA R-10, Japan), 0.4% Macerozyme R10 (Yakult, Japan) in 10 mL water. The solution was adjusted to pH to 5.7 with 1 M Tris pH 8. Add 0.1% BSA and filter using a 0.4um filter. About 120 Roots are transferred in 2ml of protoplast solution in a small petri dish(35x10mm) for 15mins at 100 rpm. As the enzyme degrades preferentially the elongation zone, when the root tips are detached, they are transferred into a new small petri dish containing 2ml of fresh protoplast solution. Root tips are incubated for 1h45 at 100 rpm at room temperature. After passing through two 20um filters placed on top of a 40 μm strainer, protoplasts were centrifuged at 500 g for 5 min and resuspended twice in washing buffer: 400 mM/8% mannitol, 20 mM MES hydrate, 10 mM KCl, 10 mM CaCl2, pH 5.7, BSA 0.1%, filtered at 0.22um. Final suspension volume was adjusted to a density of 2,000 cells/μl. Protoplasts were placed on ice until further processing.

Single Cell Sequencing

Single cell RNA sequencing was performed using 10x Genomics Single Cell 3' Kit V3 according to the manufacturer instructions. A total of 16 000 cells were loaded in the chromium for each condition. Libraries were sequenced using Illumina NextSeq 500 HighOutput on a V2.5 chip. With about 2 libraries per run and a sequencing saturation of 30-40%. Sequenced libraries were aligned on the TAIR10.38 Arabidopsis genome using the software Cellranger (v.3.0.1).

Single Cell Analysis

Sequenced cells were analyzed using the R package Seurat V3.1 version, CountClust (V), and DynRB (V). Add packrat bundle file with Seurat, DynRB, CountClust. Cells having less than 1600 genes and 10 000 UMI or more than 11 000 genes or 400 000 UMI detected were removed from the analysis as bad quality cells and potential cell doublet.

Topic Modeling

The number of suitable topics has been established using the R package dynRB to empirically identify how many topics are necessary to distinguish every cell type in the control condition with a minimum of overlap between them. Eleven topics were found to be the minimum number with the smallest overlap compared to K+1 (supplementary Fig 59566, 08632), whereas any more than 11K appears to overfit the model.

Silhouette Analysis

Silhouette analysis revealed that cells with a high topic 4 level have a significantly lower silhouette score when compared against other cells from either the uncut or cut conditions, suggesting they are indeed more different than the other cells that compose each cluster. Finally when we look at the second closest cluster to which cells could have been assigned, cells having a high topic 4 level are more likely to be assigned LRC or columella identity than cells from the uncut condition, suggesting that these cells indeed have a more mixed identity than other cells.
To confirm, we used the more standard Seurat alignment workflow based on Variance Stabilizing Transformation (VST) and log normalization. This approach led to the emergence of an ectopic cluster only present in cut roots (suppl 08633). The 1,799 cells composing this novel group are extremely enriched in cluster 4 and 88% of them are present in our CountClust approach while also displaying a much lower silhouette score. While Seurat was only able to identify 1,799 cells—potentially simply ones with the strongest transcriptomic signature—the topic modeling approach was able to identify about 3,677 cells, potentially capturing more subtle transcriptional changes.

References

Aquea F, Timmermann T, Herrera-Vásquez A. 2017. Chemical inhibition of the histone acetyltransferase activity in Arabidopsis thaliana. *Biochem Biophys Res Commun* **483**:664–668.

Balasubramanyam K, Varier RA, Altaf M, Swaminathan V, Siddappa NB, Ranga U, Kundu TK. 2004. Curcumin, a novel p300/CREB-binding protein-specific inhibitor of acetyltransferase, represses the acetylation of histone/nonhistone proteins and histone acetyltransferase-dependent chromatin transcription. *J Biol Chem* **279**:51163–51171.

Bargmann BOR, Birnbaum KD. 2010. Fluorescence activated cell sorting of plant protoplasts. *J Vis Exp*. doi:10.3791/1673

Chen L-T, Wu K. 2010. Role of histone deacetylases HDA6 and HDA19 in ABA and abiotic stress response. *Plant Signal Behav* **5**:1318–1320.

Costa S, Shaw P. 2006. Chromatin organization and cell fate switch respond to positional information in Arabidopsis. *Nature* **439**:493–496.

Dey KK, Hsiao CJ, Stephens M. 2017. Visualizing the structure of RNA-seq expression data using grade

of membership models. *PLoS Genet* **13**:e1006599.
Dong J, MacAlister CA, Bergmann DC. 2009. BASL controls asymmetric cell division in Arabidopsis. *Cell* **137**:1320–1330.
Efroni I, Mello A, Nawy T, Ip P-L, Rahni R, DelRose N, Powers A, Satija R, Birnbaum KD. 2016. Root Regeneration Triggers an Embryo-like Sequence Guided by Hormonal Interactions. *Cell* **165**:1721–1733.
Guo S, Zi X, Schulz VP, Cheng J, Zhong M, Koochaki SHJ, Megyola CM, Pan X, Heydari K, Weissman SM, Gallagher PG, Krause DS, Fan R, Lu J. 2014. Nonstochastic reprogramming from a privileged somatic cell state. *Cell* **156**:649–662.
Harashima H, Schnittger A. 2010. The integration of cell division, growth and differentiation. *Curr Opin Plant Biol* **13**:66–74.
Hay ED, Fischman DA. 1961. Origin of the blastema in regenerating limbs of the newt Triturus viridescens. An autoradiographic study using tritiated thymidine to follow cell proliferation and migration. *Dev Biol* **3**:26–59.
Hernández-Coronado M, Dias Araujo PC, Ip P-L, Nunes CO, Rahni R, Wudick MM, Lizzio MA, Feijó JA, Birnbaum KD. 2022. Plant glutamate receptors mediate a bet-hedging strategy between regeneration and defense. *Dev Cell* **57**:451–465.e6.
Ikeuchi M, Iwase A, Rymen B, Harashima H, Shibata M, Ohnuma M, Breuer C, Morao AK, de Lucas M, De Veylder L, Goodrich J, Brady SM, Roudier F, Sugimoto K. 2015. PRC2 represses dedifferentiation of mature somatic cells in Arabidopsis. *Nat Plants* **1**:15089.
Iwakawa H, Shinmyo A, Sekine M. 2006. Arabidopsis CDKA;1, a cdc2 homologue, controls proliferation of generative cells in male gametogenesis. *Plant J* **45**:819–831.
Jenik PD, Jurkuta REJ, Barton MK. 2005. Interactions between the cell cycle and embryonic patterning in Arabidopsis uncovered by a mutation in DNA polymerase epsilon. *Plant Cell* **17**:3362–3377.
Kazda A, Akimcheva S, Watson JM, Riha K. 2016. Cell Proliferation Analysis Using EdU Labeling in Whole Plant and Histological Samples of Arabidopsis. *Methods Mol Biol* **1370**:169–182.
Kidner C, Sundaresan V, Roberts K, Dolan L. 2000. Clonal analysis of the Arabidopsis root confirms that position, not lineage, determines cell fate. *Planta* **211**:191–199.
Mac Auley A, Werb Z, Mirkes PE. 1993. Characterization of the unusually rapid cell cycles during rat gastrulation. *Development* **117**:873–883.
Meyer HM, Teles J, Formosa-Jordan P, Refahi Y, San-Bento R, Ingram G, Jönsson H, Locke JCW, Roeder AHK. 2017. Fluctuations of the transcription factor ATML1 generate the pattern of giant cells in the sepal. *Elife* **6**. doi:10.7554/eLife.19131
Motte H, Vanneste S, Beeckman T. 2019. Molecular and Environmental Regulation of Root Development. *Annu Rev Plant Biol* **70**:465–488.
Ohashi-Ito K, Bergmann DC. 2006. Arabidopsis FAMA controls the final proliferation/differentiation switch during stomatal development. *Plant Cell* **18**:2493–2505.
Orford KW, Scadden DT. 2008. Deconstructing stem cell self-renewal: genetic insights into cell-cycle regulation. *Nat Rev Genet* **9**:115–128.
Pfefferli C, Jaźwińska A. 2015. The art of fin regeneration in zebrafish. *Regeneration (Oxf)* **2**:72–83.
Pfefferli C, Müller F, Jaźwińska A, Wicky C. 2014. Specific NuRD components are required for fin regeneration in zebrafish. *BMC Biol* **12**:30.
Planchais S, Glab N, Inzé D, Bergounioux C. 2000. Chemical inhibitors: a tool for plant cell cycle studies. *FEBS Lett* **476**:78–83.
Rahni R, Birnbaum KD. 2019. Week-long imaging of cell divisions in the Arabidopsis root meristem. *Plant Methods* **15**:30.
Rosa S, Ntoukakis V, Ohmido N, Pendle A, Abranches R, Shaw P. 2014. Cell differentiation and development in Arabidopsis are associated with changes in histone dynamics at the single-cell level. *Plant Cell* **26**:4821–4833.
Rosa S, Shaw P. 2013. Insights into chromatin structure and dynamics in plants. *Biology* **2**:1378–1410.
Ruffel S, Krouk G, Ristova D, Shasha D, Birnbaum KD, Coruzzi GM. 2011. Nitrogen economics of root foraging: transitive closure of the nitrate-cytokinin relay and distinct systemic signaling for N supply vs. demand. *Proc Natl Acad Sci U S A* **108**:18524–18529.
Rymen B, Kawamura A, Lambolez A, Inagaki S, Takebayashi A, Iwase A, Sakamoto Y, Sako K, Favero

DS, Ikeuchi M, Suzuki T, Seki M, Kakutani T, Roudier F, Sugimoto K. 2019. Histone acetylation orchestrates wound-induced transcriptional activation and cellular reprogramming in Arabidopsis. *Commun Biol* **2**:404.

Sánchez Alvarado A. 2009. Developmental biology: A cellular view of regeneration. *Nature*.

Satija R, Farrell JA, Gennert D, Schier AF, Regev A. 2015. Spatial reconstruction of single-cell gene expression data. *Nat Biotechnol* **33**:495–502.

Sena G, Wang X, Liu H-Y, Hofhuis H, Birnbaum KD. 2009. Organ regeneration does not require a functional stem cell niche in plants. *Nature* **457**:1150–1153.

Sun B, Looi L-S, Guo S, He Z, Gan E-S, Huang J, Xu Y, Wee W-Y, Ito T. 2014. Timing mechanism dependent on cell division is invoked by Polycomb eviction in plant stem cells. *Science* **343**:1248559.

Tanaka M, Kikuchi A, Kamada H. 2008. The Arabidopsis histone deacetylases HDA6 and HDA19 contribute to the repression of embryonic properties after germination. *Plant Physiol* **146**:149–161.

Tian L, Fong MP, Wang JJ, Wei NE, Jiang H, Doerge RW, Chen ZJ. 2005. Reversible histone acetylation and deacetylation mediate genome-wide, promoter-dependent and locus-specific changes in gene expression during plant development. *Genetics* **169**:337–345.

Trichostatin A. n.d. doi:10.1016/bs.armc.2019.06.004

Truernit E, Bauby H, Dubreucq B, Grandjean O, Runions J, Barthélémy J, Palauqui J-C. 2008. High-resolution whole-mount imaging of three-dimensional tissue organization and gene expression enables the study of Phloem development and structure in Arabidopsis. *Plant Cell* **20**:1494–1503.

Tsubouchi T, Fisher AG. 2013. Reprogramming and the pluripotent stem cell cycle. *Curr Top Dev Biol* **104**:223–241.

Ueda M, Matsui A, Tanaka M, Nakamura T, Abe T, Sako K, Sasaki T, Kim J-M, Ito A, Nishino N, Shimada H, Yoshida M, Seki M. 2017. The Distinct Roles of Class I and II RPD3-Like Histone Deacetylases in Salinity Stress Response. *Plant Physiol* **175**:1760–1773.

von Wangenheim D, Hauschild R, Fendrych M, Barone V, Benková E, Friml J. 2017. Live tracking of moving samples in confocal microscopy for vertically grown roots. *Elife* **6**. doi:10.7554/eLife.26792

Weigel D, Jürgens G. 2002. Stem cells that make stems. *Nature* **415**:751–754.

Zhou C, Zhang L, Duan J, Miki B, Wu K. 2005. HISTONE DEACETYLASE19 is involved in jasmonic acid and ethylene signaling of pathogen response in Arabidopsis. *Plant Cell* **17**:1196–1204.

Zhukovskaya NV, Bystrova EI, Dubrovsky JG, Ivanov VB. 2018. Global analysis of an exponential model of cell proliferation for estimation of cell cycle duration in the root apical meristem of angiosperms. *Ann Bot* **122**:811–822.

Figure 1

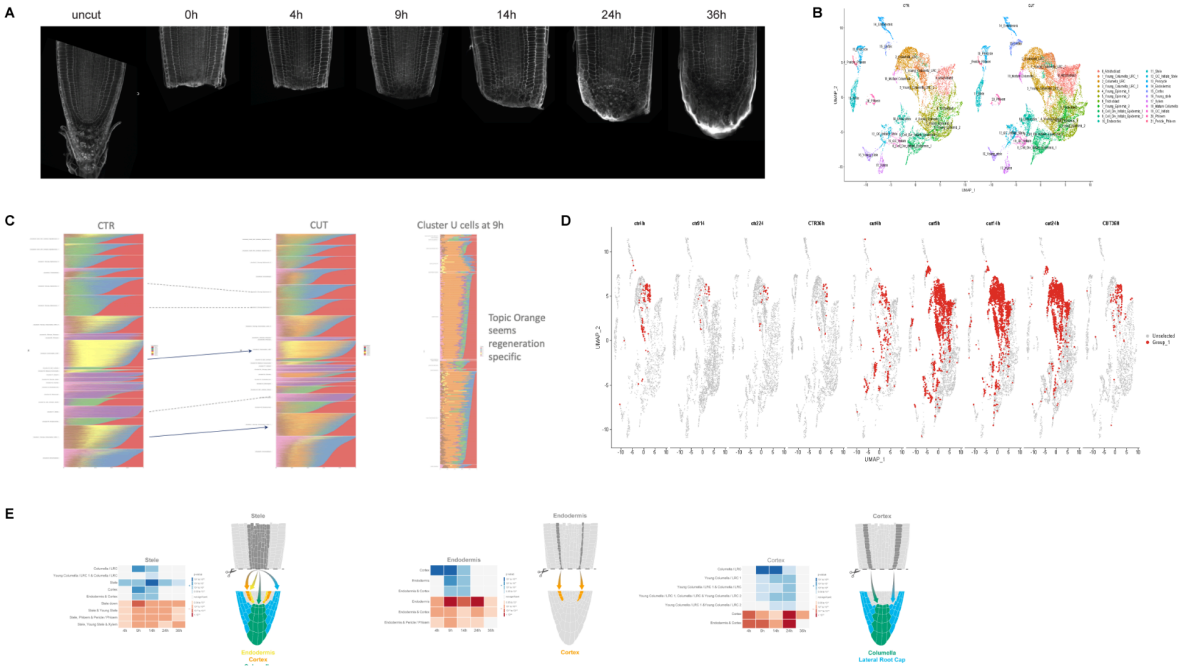

Figure 1. Topic modeling identifies cells undergoing regenerative reprogramming. (a) mPS-PI time series of a regenerating root. (b) UMAP of cut vs uncut root with different cell types in different colors. (c) Topic modeling reveals a distinct regeneration-specific identity, in orange. (d) UMAP showing the tissues enriched for orange topic cells over time. (e) Heatmaps and schematics showing which tissues leftover stele, endodermis, and cortex give rise to in the regenerating root.

Figure 2

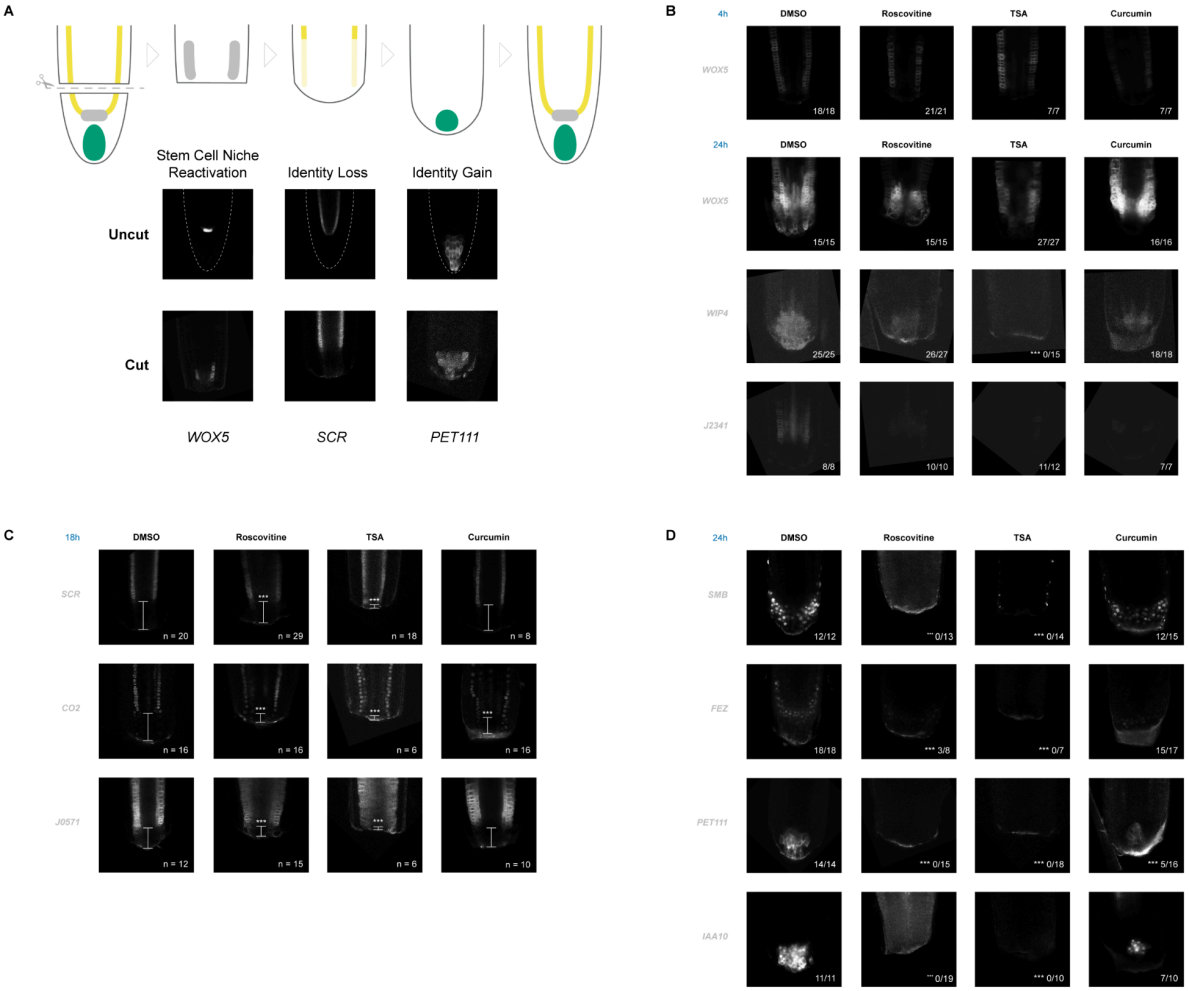

Figure 2. Division and chromatin remodeling affect different stages of regeneration. (a) Top: Schematic showing the three stages of regeneration: ectopic activation of stem cell niche markers (gray), loss of old identity (yellow), and gain of new identity (green). Bottom: Confocal images of pWOX5:GFP, pSCR:YFP, and PET111:GFP in uncut and cut roots, corresponding to the three schematic stages. (b) Confocal images of stem cell niche markers in uncut and cut roots after mock, Roscovitine, TSA, and Curcumin treatment. (c) Confocal images of remnant markers in uncut and cut roots after mock, Roscovitine, TSA, and Curcumin treatment. (d) Confocal images of cap markers in uncut and cut roots after mock, Roscovitine, TSA, and Curcumin treatment.

Figure 3

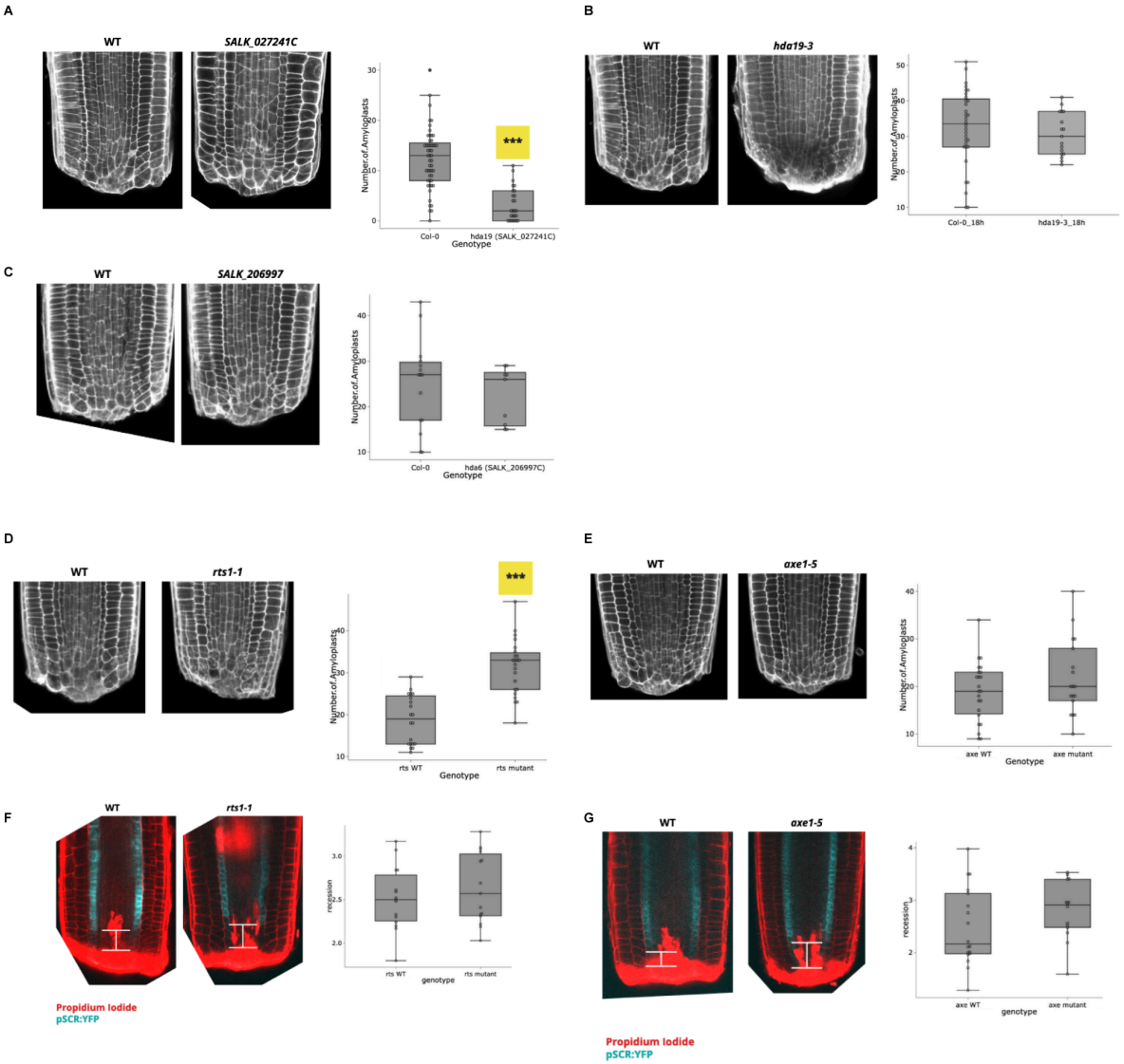

Figure 3. Histone deacetylase activity affects root regeneration. a) Left: mPS-PI stained roots of Col-0 WT vs *hda19 (SALK_027241)* mutants. Right: Box plot with jitter showing quantification of amyloplast-positive cells in each genotype. *** $p < 0.005$. (b) Left: mPS-PI stained roots of Col-0 WT vs *hda19-3* mutants. Right: Box plot with jitter showing quantification of amyloplast-positive cells in each genotype. (c) Left: mPS-PI stained roots of Col-0 WT vs *hda6 (SALK_206997)* mutants. Right: Box plot with jitter showing quantification of amyloplast-positive cells in each genotype. (d) Left: mPS-PI stained roots of WT siblings vs *hda6 (rts1-1)* mutants. Right: Box plot with jitter showing quantification of amyloplast-positive cells in each genotype *** $p < 0.005$. (e) Left: mPS-PI stained roots of WT siblings vs *hda6 (axe1-5)* mutants. Right: Box plot with jitter showing quantification of amyloplast-positive cells in each genotype. (f) Left: PS-PI stained roots of WT siblings vs *hda6 (rts1-1)* mutants expressing a transcriptional reporter for *SCR (pSCR:YFP)*. Right: Box plot with jitter showing distance from cut site to edge of *SCR* fluorescence domain. (g) Left: PS-PI stained roots of WT siblings vs *hda6 (axe1-5)* mutants expressing a transcriptional reporter for *SCR (pSCR:YFP)*. Right: Box plot with jitter showing distance from cut site to edge of *SCR* fluorescence domain.

Figure 4

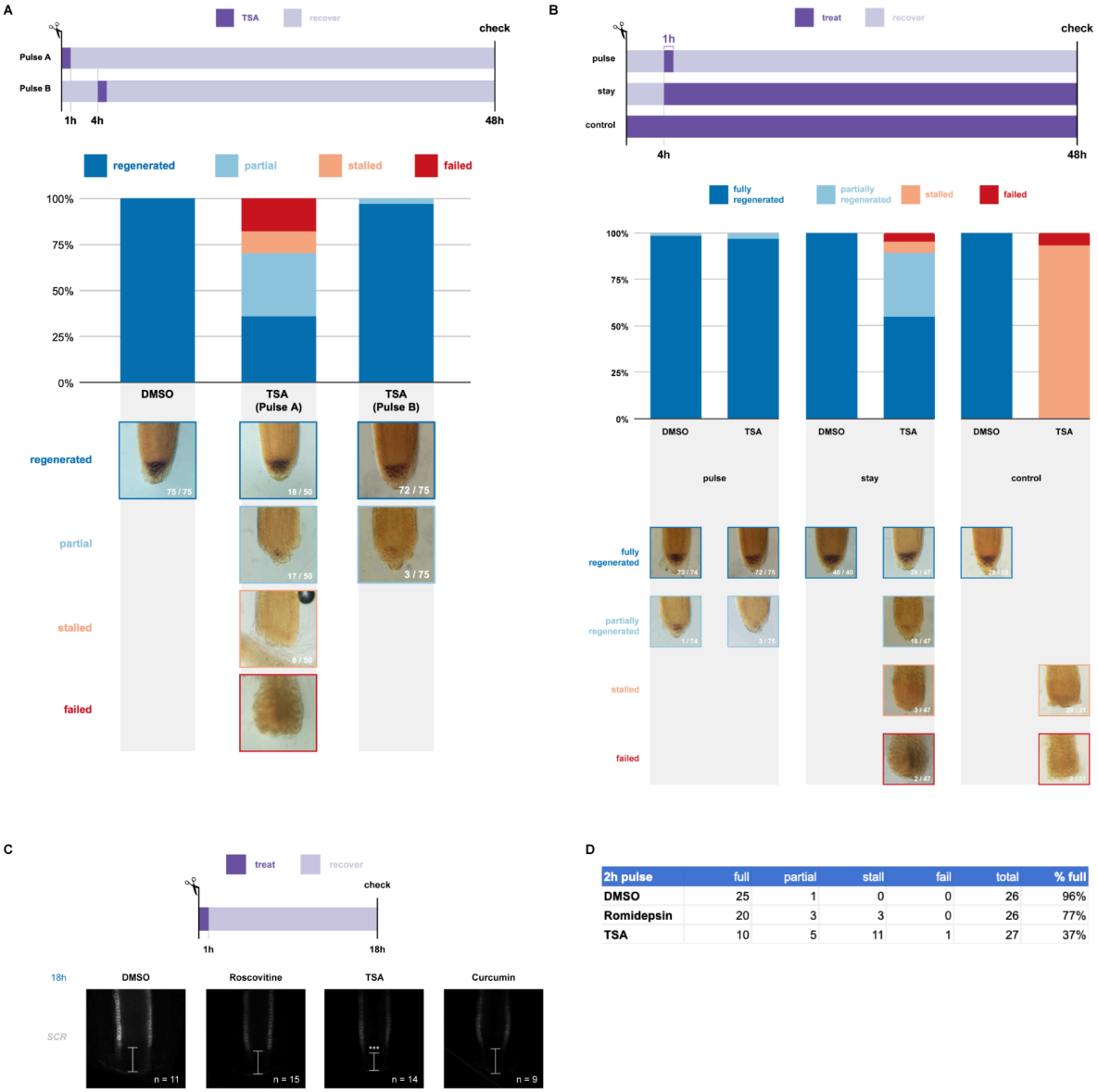

2h pulse	full	partial	stall	fail	total	% full
DMSO	25	1	0	0	26	96%
Romidepsin	20	3	3	0	26	77%
TSA	10	5	11	1	27	37%

Figure 4. Histone deacetylase activity is needed in the first hour after wounding. (a) Top: Experimental scheme—plants were cut and either treated with TSA immediately after for 1h (Pulse A), or given a 1h pulse 4h post cut (Pulse B). Roots were then stained with lugol at 48h post cut to visualize amyloplasts, as a proxy for reprogramming. An immediate 1h pulse significantly perturbs regeneration. (b) Waiting 4 hours before delivering a 1h pulse of TSA does not have a significant impact on regeneration compared to keeping them on TSA 4h post cut or keeping them on TSA the entire time. (c) A 1h pulse of TSA immediately after cutting also affects loss of old identities, as seen by less disappearance of *pSCR:YFP* near the cut site compared to mock, Roscovitine, or Curcumin. (d) A 2h pulse of Romidepsin has a moderate, but not statistically significant, affect on regeneration, whereas a 2h pulse of TSA has a significant impact.

Supplemental Figure 1

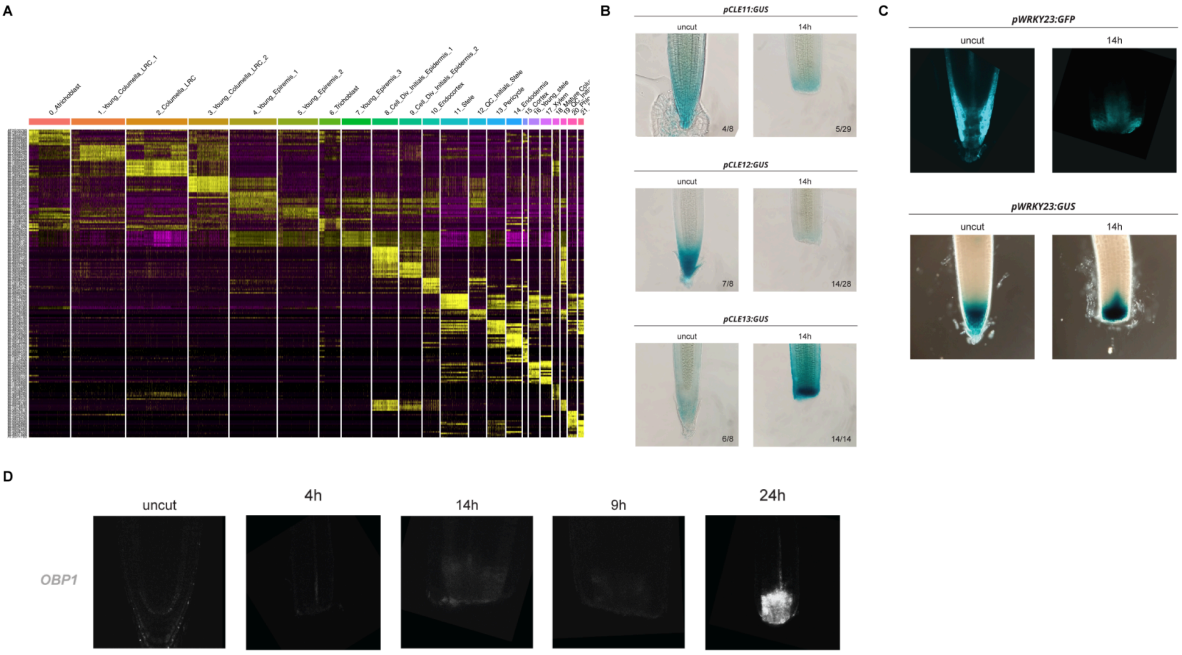

Supplemental Figure 1. Identifying early stage regeneration markers. (a) Heatmap of top ten cell type-specific markers in uncut roots. (b) GUS staining of uncut and 14h cut roots showing the localization of CLE11, 12, and 13 gene expression. (c) pWRKY23:GFP and GUS imaging of WRKY23 in uncut and 14h cut roots. (d) Confocal imaging of uncut and cut pOBP1:RFP reporter over time.

Supplemental Figure 2

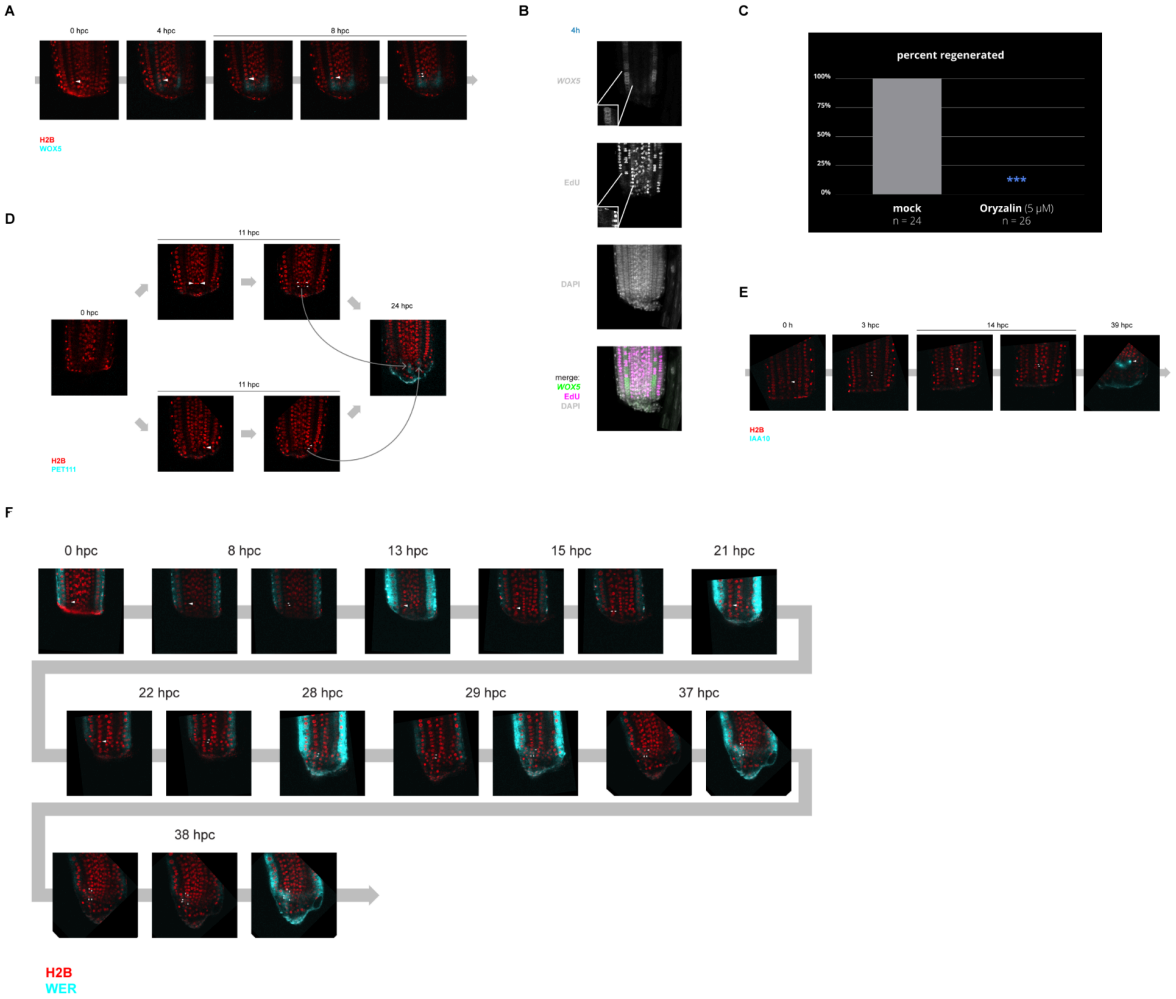

Supplemental Figure 2. The reappearance of different cell identity markers have varied dependencies on cell division. (a) Still images from time-lapse movie showing *WOX5* expression returning before cell division in a regenerating root. (b) Co-labeling of a *WOX5* transcriptional reporter with EdU in a 4h cut root showing mutually exclusive domains. (c) Bar plot showing failure to regenerate when roots are treated with the cell cycle inhibitor Oryzalin. (d) Still images from time-lapse movie showing the return of PET111 expression during regeneration occurring after cells have already divided. (e) Still images from time-lapse movie showing *IAA10* expression during regeneration returning only after cells have already divided. (f) Still images from time lapse movie showing *WEREWOLF* expression during regeneration returning to the lateral root cap only after cells have already divided.

Supplemental Figure 3

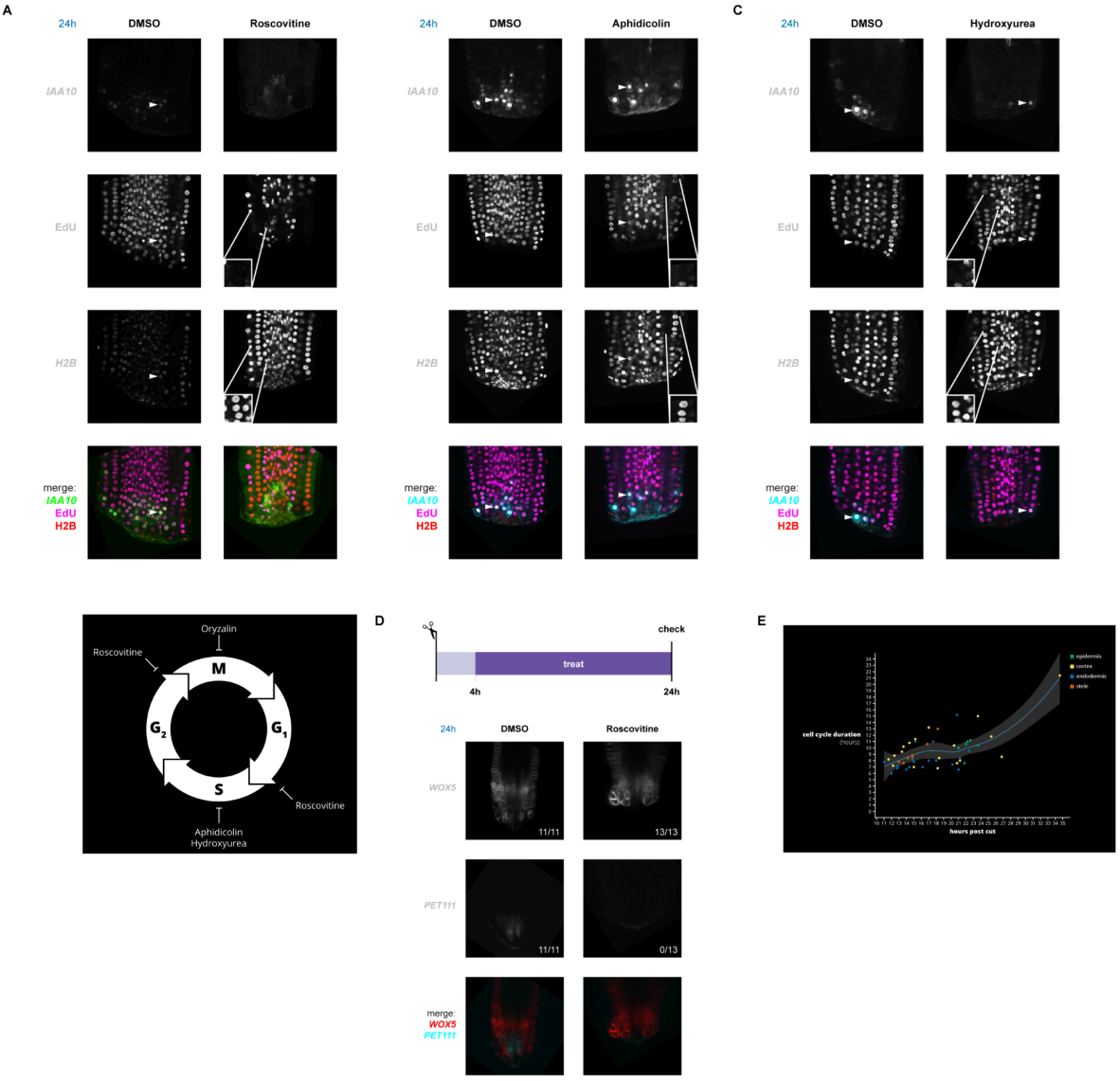

Supplemental Figure 3. Different markers under various cell cycle inhibitors and division rates in regeneration. Confocal images of *pIAA10:3x-NLS-GFP*, *p35S:H2B-mCherry*, and EdU labeling after cell cycle inhibition with (a) Roscovitine, (b) Aphidicolin, and (c) Hydroxyurea. Return of *IAA10* expression only occurs in EdU-positive cells. (d) Cutting roots, waiting 4 hours, then transferring to mock or Roscovitine treatment blocks regeneration, as seen by the absence of PET111, whereas *WOX5* expression is not affected. (e) Scatterplot showing cell cycle duration for different cells during regeneration, as observed in time lapse movies. Compared to uncut roots, the average cell cycle duration is nearly three-fold faster.

Supplemental Figure 4

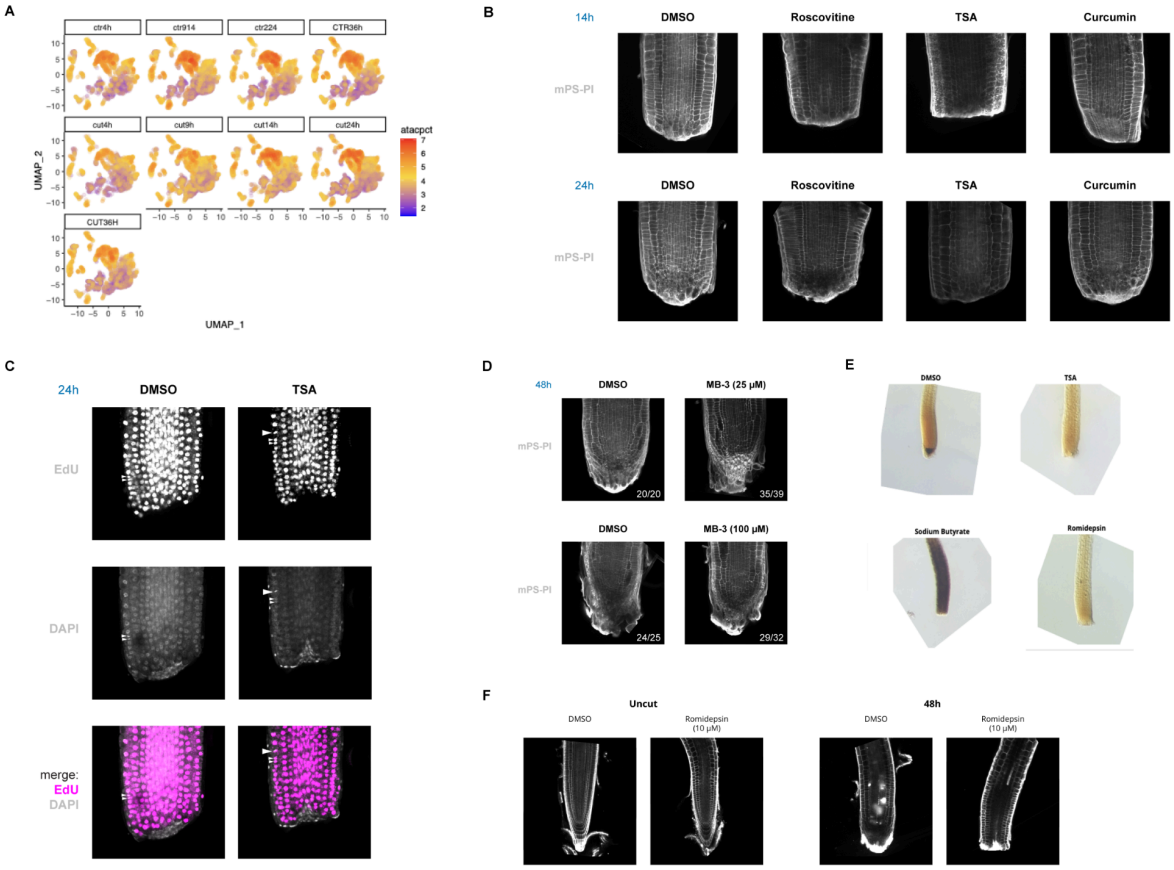

Supplemental Figure 4. Effect of treatments on amyloplast recovery and effect of TSA on cell division. (a) UMAPs showing open chromatin regions from ATAC-seq data in uncut (ctr) and cut roots at different time points. (b) mPS-PI staining showing the effects of Roscovitine, TSA, and Curcumin treatment compared to mock at 14 and 24h. (c) EdU labeling of TSA-treated roots showing that S phase entry is not affected compared to mock. Mitotic figures are visible in both conditions, suggesting that cell division is not significantly affected by TSA treatment. (d) mPS-PI staining of roots treated with the HAT inhibitor MB-3. While there are some morphological differences between mock and treat, roots are able to regenerate in both conditions, as seen by the return of amyloplast-positive cells at 48h. (e) Brightfield images of lugol-stained roots 48h post cut in mock, TSA, Sodium Butyrate, and Romidepsin conditions. (f) PI staining of uncut and cut roots treated with mock or Romidepsin, highlighting the treated roots' similarities to TSA-treated roots (panel B)

Supplemental Figure 5

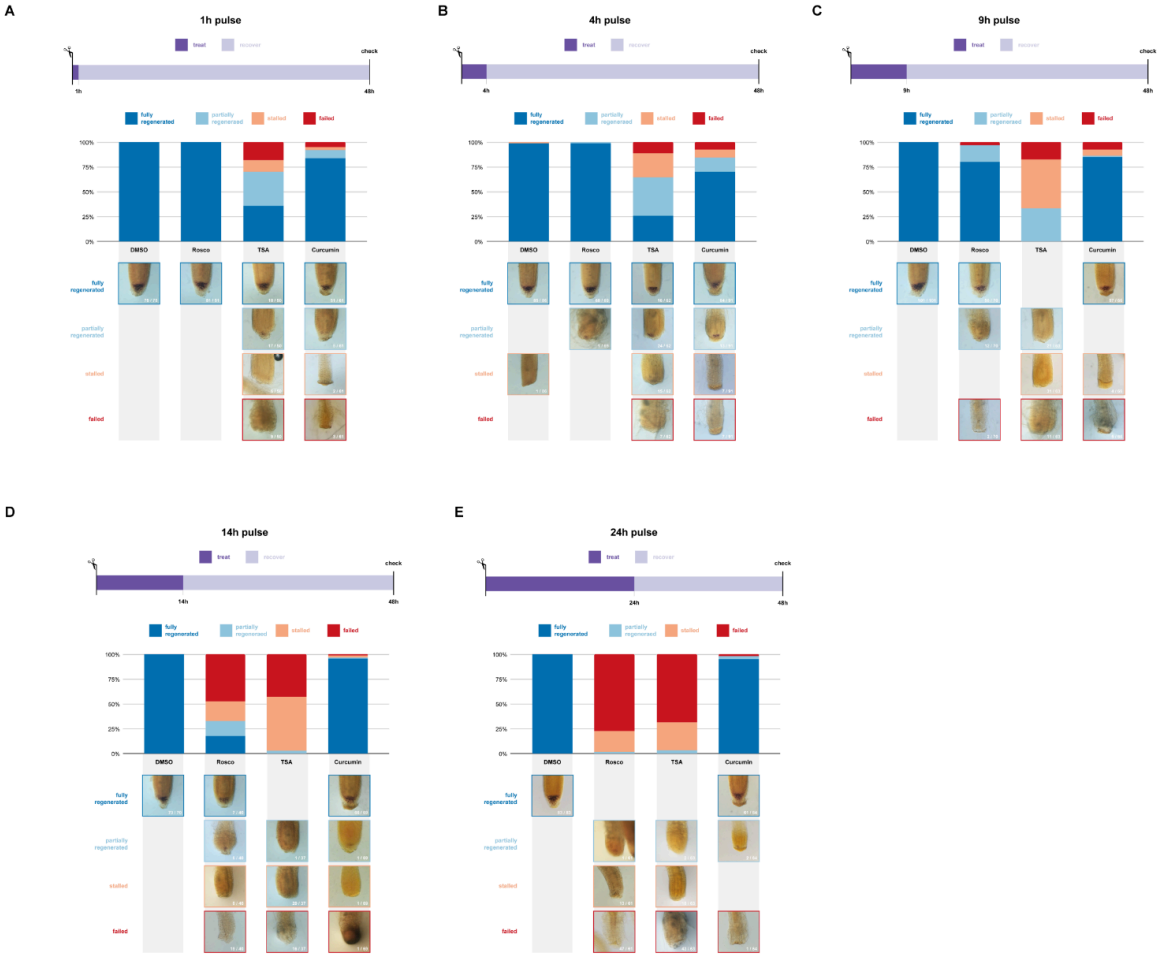

Supplemental Figure 5. Root regeneration is sensitive to perturbation of histone deacetylases in short treatment windows. (a-e) Roots were cut and plants transferred to (a) 1h, (b) 4h, (c) 9h, (d) 14h, and (e) 24h pulses of TSA, Roscovitine, or Curcumin, then stained with Lugol at 48h post cut to visualize amyloplasts, as a proxy for reprogramming. Increasing the pulse duration has a more dramatic effect but only TSA shows a significant effect in shorter pulses.